JCTC Journal of Chemical Theory and Computation

Article

pubs.acs.org/JCTC

Toward Accurate Modeling of the Effect of Ion-Pair Formation on Solute Redox Potential

Xiaohui Qu and Kristin A. Persson*

Energy Technologies Area, Lawrence Berkeley National Laboratory, Berkeley, California 94720, United States

ABSTRACT: A scheme to model the dependence of a solute redox potential on the supporting electrolyte is proposed, and the results are compared to experimental observations and other reported theoretical models. An improved agreement with experiment is exhibited if the effect of the supporting electrolyte on the redox potential is modeled through a concentration change induced via ion pair formation with the salt, rather than by only considering the direct impact on the redox potential of the solute itself. To exemplify the approach, the scheme is applied to the concentration-dependent redox potential of select molecules proposed for nonaqueous flow batteries. However, the methodology is general and enables rational computational electrolyte design through tuning of the operating window of electrochemical systems by shifting the redox potential of its solutes; including potentially both salts as well as redox active molecules.

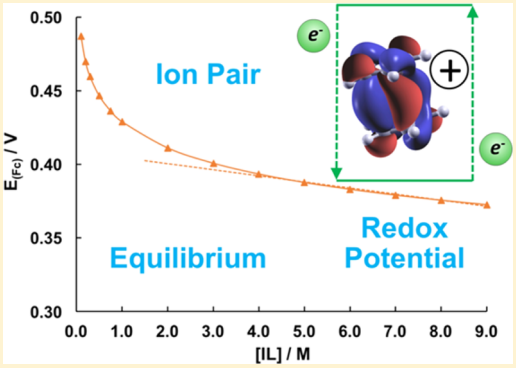

1. INTRODUCTION

The concept of ion pair formation was first proposed by Bjerrum in the 1920s and describes the local association of oppositely charged ions in electrolyte solutions.[1,2] Since then, support of this concept has derived from both experimental and computational work.[2−6] While ion pairing is typically weak in aqueous solutions, it is more pronounced in organic electrolytes and shows a strong dependence on concentration.[3,5] Generally, ion-pairing can occur between any two oppositely charged ions in solution, and its occurrence can have significant consequences on the properties of the electrolyte.[2,3,7−14] For example, a strong effect of the electrolyte on the electrochemical reduction of cyclooctateraene was attributed to ion pairing.[15] Very strong ion-pairing in an aqueous electrolyte was recently shown to significantly increase the operating voltage of an energy storage system from the nominal aqueous stability window of 1.6 V to almost 3 V.[16] Ion-pairing can also have detrimental effects as shown in refs 3 and 17 wherein a salt decomposition mechanism during charge transfer was coupled to the ion-paired solvation structure of the electrolyte.

While it has been shown that the redox potential of an electrolyte can be tuned by varying the anion component of the salt,[9] there is no consensus on how to accurately model the redox potential of a charged solute in the close proximity of oppositely charged species. For example, a *direct calculation* of the electron affinity or the ionization potential of a solute by itself as well as in an ion-paired configuration provides an initial guide to the change in the redox potential as a function of ion-pairing.[3,10,18] Maeshima et al. found reasonable agreement for capacitor electrolyte systems[10] using the direct method, and furthermore reported an improved version which considered the redox potentials of isolated ions, ion pairs, solvent molecule, and used the redox potential of the most reactive specie as the final result.[11] Haskins et al. studied the electrochemical anodic stability (ionization energy) of a lithium-doped ionic liquid using ab initio calculations and found that the calculation of the ionization potential of the interacting cation/anion pairs provided a lower and upper bound, respectively, to the experimental data.[12]

As early as 1975, the reduction potential of aromatic hydrocarbon was found to be significantly affected by the salt concentrations in tetrahydrofuran solutions.[19] Continuum models have also been proposed where the change to the solute redox potential is assumed to be mediated by a change in its solvation energy.[13,20,21] For example, Seto et al. measured the redox potential of a series of salt concentrations and proposed to explain the salt concentration dependence on the observed potential of the redox active species by assuming that the anion/cation changes the dielectric constant of the solution, and as a result, impacts the solvation energy of the redox active solute. This approach was tested on benzoquinone[22] in a supporting ionic liquid, where the effect of salt concentration was modeled via a dielectric continuum solvation model[23,24] calibrated by the calculated dielectric constants. Torriero et al. measured the dependence of the ferrocene redox potential on the supporting ionic liquid concentration.[25] While both reports observed a logarithmic relationship within the concentration range from 0.1 to 1.0 M, there were some important differences. Approaching neat conditions (≥1.0 M), Seto et al. reported an asymptotic plateau, however, Torriero observed a linear relationship between the redox potential and the ionic liquid concentration.

Received: March 22, 2016
Published: August 8, 2016

DOI: 10.1021/acs.jctc.6b00289
J. Chem. Theory Comput. 2016, 12, 4501−4508

By construction, the direct method is likely to overestimate the effect of the ion-pairing, as it neglects equilibrium concentration shifts from the change in population between the ion-pair and free solute species. Conversely, a continuum approach lacks information about the local charge redistribution in the solute as a function of the ion-pairing. In this paper, we present a new approach, namely the ion-pair equilibrium (IPE) model, that captures the influence of the ion-pair formation on the redox potential of a redox active molecule by *incorporating the direct effect through a change in the equilibrium concentration of the redox active species*. We present results for three representative systems, where two allow for benchmarking with existing experiments taken from the literature.

2. COMPUTATIONAL METHODS

We propose that, for systems where ion pair formation between the redox active solution and a counterion is expected, the redox potential is changed as a result of the concentration change of the redox active solute, potentially both in its charged as well as discharged state. The source of counterions generally includes salts, additives, ionic liquids, and other components that comprise cations/anions. We simulate the concentration dependence by computing the thermodynamic properties from *ab initio* calculations using the following procedure: (1) the ion-pair dissociation constants are determined from the ion-pair Gibbs free reaction energy, which, in turn, is calculated using density functional theory (DFT);[26,27] (2) the concentration change of the redox active solute is obtained via a simple chemical equilibrium model; (3) the redox potential at the standard potential is computed using DFT calculations; and finally, (4) the concentration dependence of the redox potential is deduced from the Nernst equation using the results from step 1−3. All Density Functional Theory (DFT) calculations are performed using the QChem 4.3 quantum mechanical software package.[28,29] The calculation of the dissociation constants and redox potential are automated using an in-house developed high-throughput infrastructure.[30,31] Dispersion corrections for noncovalent interactions are obtained through Grimme's D3 functional.[32,33] All geometries are optimized at the B3LYP-D3/6-31+G(d) theoretical level, and the harmonic vibration frequencies are calculated at the same level to determine the Gibbs free energies (ΔG). The single point energies are evaluated using a larger basis set at the B3LYP-D3/6-311++G(d,p) level to improve the accuracy of the energy evaluations.[34] The SRSC "small-core" effective core potential is used for iron-containing species to take relativistic effects into account[35] and the solvation energy is calculated through the dielectric continuum model IEF-PCM.[36] In the case of mixed solvents, a composite dielectric constant is calibrated from the dielectric constants of pure components using an empirical model[37] derived from the Kirkwood theory for multicomponent systems.[38]

As a measure of the tendency to gain/loose electrons, the redox potential is expressed by either a reduction potential or an oxidation potential with reference to a standard electrode. Generally, this terminology results in two ways to write half-cell reactions: an oxidation reaction and a reduction reaction. In this paper, we follow the IUPAC convention such that the species in question is being reduced,[39,40] that is, all the redox potentials refer to the reduction reaction if not explicitly specified.[39,40]

2.1. Calculation of Dissociation Constants. We assume that the electrolyte is well solvated, that is, that the supporting electrolyte salt and redox active solute can exist either as dissociated free ions or contact ion pairs (CIP).[41,42] At higher salt and solute concentrations, clusters and ion-pair percolation paths can form;[16,43] however, this is beyond the scope of this paper. As already mentioned, the specifics of the ion-pairing depend on the original charged state of the redox active solute, and what redox processes (reduction and/or oxidation) it undergoes in solution. For example, if the charged state is an anion the ion-pair will involve a cation from the supporting electrolyte and the oxidation potential of the solute will be changed as a result of the concentration change of the non ion-paired, "free" solute. Conversely, if the solute is a cation, the ion-pair will include a negatively charged ion from solution (e.g., a salt anion) and this will shift the reduction potential downward for the ion-pair. While our methodology is applicable to any of these scenarios, for transparency we choose to outline our procedure assuming an originally neutral redox-active solute which undergoes oxidation. If we use R^+ to denote the resulting cation and A^- to denote the supporting electrolyte anion, the dissociation of the ion pair can be represented by the following reaction:

$$R^+A^- \rightleftharpoons R^+ + A^-$$

The dissociation constant can be expressed in terms of mole concentrations:

$$K_e = \frac{c_{R^+} \cdot c_{A^-}}{c_{R^+A^-}} \tag{1}$$

in which, c_{R^+}, c_{A^-} and $c_{R^+A^-}$ are the concentrations of the cation, anion, and ion pair, respectively, and K_e can be related to the standard-state Gibbs free reaction energy by

$$\Delta G^\circ = -RT \ln K_e \tag{2}$$

where R is the ideal gas constant and T is the temperature. In this work, room temperature (298.15 K) is assumed if not otherwise explicitly specified. ΔG° is the standard-state Gibbs free reaction energy and can be evaluated from DFT calculations:

$$\Delta G^\circ = G_{R^+} + G_{A^-} - G_{R^+A^-}$$

2.2. A Chemical Equilibrium Model To Determine the Concentration of "Free" Redox Active Molecules. We denote the initial concentrations of the redox active solute and electrolyte salt as $c_{0,R}$ and $c_{0,A}$, respectively. For the redox active solute, we assume an initial concentration of $c_{0,R}$ and denote x as the concentration of the ion pair. Because the electrolyte salt and redox active solute can exist either as free solutes or as ion pairs, the total concentration is a summation of the two:

$$\begin{aligned} c_{0,R} &= c_{R^+} + x \\ c_{0,A} &= c_{A^+} + x \end{aligned} \tag{3}$$

Combining with eq 1, we obtain

$$K_e = \frac{(c_{0,R} - x)(c_{0,A} - x)}{x} \tag{4}$$

and by rearranging eq 4, we obtain

$$x^2 - (K_e + c_{0,R} + c_{0,A}) \cdot x + c_{0,R} \cdot c_{0,A} = 0 \tag{5}$$

Here, K_e can be deduced from DFT energies using the method discussed in section 2.1. $c_{0,R}$ and $c_{0,A}$ are known quantities, and therefore, x can be determined by solving eq 5. Now we can calculate the concentration of the "free" redox active solute as

DOI: 10.1021/acs.jctc.6b00289
J. Chem. Theory Comput. 2016, 12, 4501−4508

$$c_{R^+,\mathrm{free}} = f_{\mathrm{free},R^+}(c_{0,R}, c_{0,A}) = c_{0,R} - x \quad (6)$$

2.3. The Redox Potential Calculation and Its Concentration Dependence. The redox potential at standard state is computed from an adiabatic ionization potential (for the redox couple with its oxidized state) or electron affinity (for the redox couple with its reduced state) calculation using DFT, which is described in detail in our previous paper.[30,31] From the Nernst equation, we have

$$E_{\mathrm{red}} = E^{\circ}_{\mathrm{red}} + \frac{RT}{zF} \ln \frac{\alpha_{\mathrm{ox}}}{\alpha_{\mathrm{red}}}$$

where z is the number of electrons transferred in the half reaction, and α_{ox} and α_{red} are the chemical activities of the oxidized and reduced species, respectively. In this work, we assume activity coefficients of 1.0 if not explicitly specified, but this can be easily generalized through:

$$\alpha_{\mathrm{ox}} = \gamma_{\mathrm{ox}} \cdot c_{\mathrm{ox}}$$

$$\alpha_{\mathrm{red}} = \gamma_{\mathrm{red}} \cdot c_{\mathrm{red}}$$

in which γ is the activity coefficient and c is the concentration. From eq 6, we write the redox potential as a function of the concentrations of the redox active solute in the oxidized ($c_{R^+,\mathrm{free}}$) and the reduced ($c_{0,R}$) state, respectively:

$$E_{\mathrm{red}} = E^{\circ}_{\mathrm{red}} + \frac{RT}{zF} \ln \frac{c_{\mathrm{ox}}}{c_{\mathrm{red}}}$$

$$= E^{\circ}_{\mathrm{red}} + \frac{RT}{zF} \ln \frac{c_{R^+,\mathrm{free}}}{c_{0,R}}$$

$$= E^{\circ}_{\mathrm{red}} + \frac{RT}{zF} \ln \frac{f_{\mathrm{free},R^+}(c_{0,R}, c_{0,A})}{c_{0,R}} \quad (7)$$

We note that eq 7 is used to calculate the redox potential *at each point* as a function of the variation in the initial electrolyte salt ($c_{0,R}$) and redox active solute ($c_{0,A}$) concentration.

3. RESULTS AND DISCUSSION

Three model systems were chosen to exemplify the suggested approach. Two systems have been previously studied experimentally and the potential-concentration dependence established, while—to the best of our knowledge—no such report exists for the third system, neither experimentally nor theoretically. The molecular structures for the relevant compounds are shown in Figure 1. The electrolyte concentration dependence of the $Fc^0/^+$ redox couple was measured by Torriero and co-workers[25] using two different ionic liquid salts: (1) 1-methyl-1-butylpyrrodilinium dicyanamide, denoted as [bmpyr][DCA]; (2) 1-methyl-1-propylpyrrolidinium bis-(fluorosulfonyl)amide, denoted as [pmpyr][FSI].[25] In both systems, dichloromethane is used as the solvent and $DmFc^0/^+$ is used as the reference electrode. The redox potential of $Fc^0/^+$ redox couple against $DmFc^0/^+$ was measured while varying the concentration of [bmpyr][DCA] and [pmpyr][FSI]. The redox active molecule of the third system, DBBB, was originally proposed by Zhang and co-workers[44] and subsequently utilized for organic redox flow batteries.[8] Here we predict the dependence of redox potential to oxidize DMB (a slightly simplified version of DBBB, chosen for computational efficiency) as a function of the electrolyte concentration in

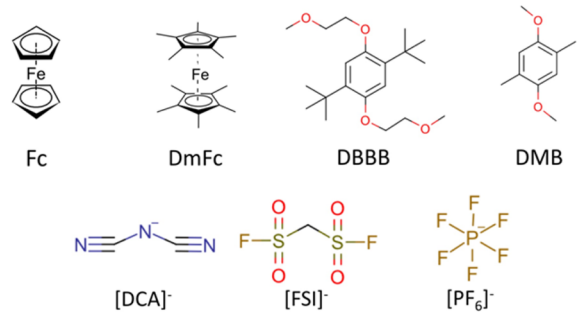

Figure 1. Structures of the redox active species and anions relevant for ion pair formation considered as examples of the proposed methodology. Abbrevations: Fc, ferrocene/ferrocenium, which are abbreviated as Fc^0 and Fc^+, respectively, in this work; DmFc, decamethylferrocene/decamethylferrocenium—$DmFc^0$ for decamethylferrocene, $DmFc^+$ for decamethylferrocenium; DBBB, 2,5-di-*tert*-butyl-1,4-bis(2-methoxyethoxy)benene; DMB, 2,5-dimethyl-1,4-bis(2-methoxy)benene; DCA, dicyanamide; FSI, bis-(fluorosulfonyl)amide; PF_6, hexafluorophosphate.

LiPF6/EC:EMC, similar to the system reported by Zhang et al.[44]

3.1. The Redox Potential at Standard State. We computed the ionization potential by DFT using both the "free" redox active molecule and the ion pair. At the B3LYP-D3/6-31+G* level, the reduction potential of the $Fc^0/^+$ redox pair in the "free" molecule state is obtained as 0.18 V versus the standard hydrogen electrode (SHE). For the same redox pair, the potential is obtained as −0.37 V versus SHE when ion paired with FSI, and −0.15 V versus SHE when ion paired with DCA. The binding of the electrolyte anion decreases the oxidation potential by 0.55 and 0.33 V, respectively. This effect can be intuitively explained by electrostatic interactions such that the close association with the negative charge from the ion-paired anion facilitates the removal of an electron from the ion-paired complex, and conversely, renders it harder to reduce. Vice versa, ion-pair formation between a redox active anion and a cation from the supporting electrolyte will generally increase the redox potential. See Figure 2 for a schematic illustration of the ion-pair effect with an anion/cation, respectively. Similar trends have been observed in other computational work.[11,12] The potential change induced by FSI is larger than that for DCA. We speculate that this is due to FSI being a geometrically more flexible molecule; and as a result, the ferrocene is allowed closer contact. Indeed, nearest neighboring cation−anion atoms in the $[Fc^+-FSI^-]$ ion pair as compared to $[Fc^+-DCA^-]$ ion pair are found at 2.16 and 2.35 Å, respectively. Hence, it can be expected that FSI will exhibit stronger influence on the Ferrocene.

At the equilibrium state, species with higher redox potentials will be reduced prior to species with lower potentials. Because free Fc^+ exhibits a higher reduction potential than that of the ion-paired complex, it will get reduced first, and accordingly shift the concentration through the equilibrium reaction between the ion-paired and the free solute populations. Similar effects are expected for other similar redox active solutes, which exist as neutral and charged cation species such as $DMB^0/^+$. As a result, in this work we will use the "free" redox active solute to calculate the reduction potential at standard state. However, we emphasize that other scenarios can exist and that the methodology is general. For example, if the active specie is a salt anion which is an ion-pair with its respective salt cation,[3]

DOI: 10.1021/acs.jctc.6b00289
J. Chem. Theory Comput. 2016, 12, 4501−4508

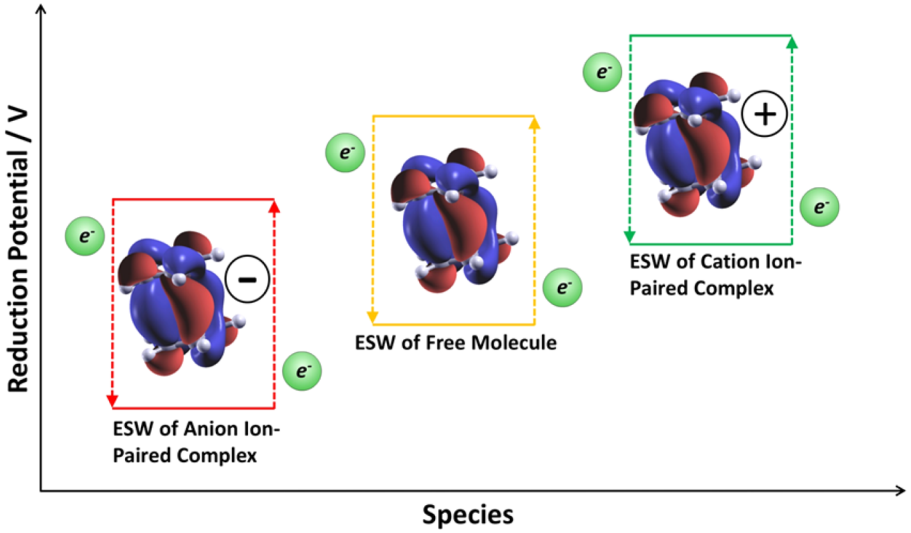

Figure 2. Schematic illustration of the qualitative effect of ion-pair formation on the electrochemical stability window (ESW, oxidation and reduction limit of the redox potential).

the ion-pair is more electropositive than the "free" anion, and hence the ion-pair will reduce at higher potentials (see Figure 2) and should be considered the active species in the following framework.

Using the same theoretical methods, the predicted reduction potential of $DmFc^+$ was obtained as −0.37 V versus SHE and the relative redox potential of $Fc^0/^+$ versus $DmFc^0/^+$ as 0.18 − (−0.37) = 0.57 V, which is in excellent agreement with the experimental value reported by Torriero et al. ranging from 0.475 V to 0.589 V. We caution that we normally expect larger errors, considering the accuracy of B3LYP functional alone.[30]

3.2. Gibbs Free Energy of Dissociation and Dissociation Constants. The driving force for ion pair association can be simulated by calculating the dissociation constant, which, in turn, can be derived from the Gibbs free energy of the ion-pair formation reaction. We calculate the Gibbs free energy of the ion-pair dissociation at the B3LYP-D3/6-311++G**//B3LYP-D3/6-31+G* level. In principle, $DmFc^+$ can also exhibit ion pair formation. However, it has been reported that $DmFc^0/^+$ is an order magnitude less sensitive to the choice of electrolyte,[25,45] and therefore, only Fc^+ is included in the potential-concentration dependence calculation.

From the enthalpy and entropy predicted by DFT, the Gibbs reaction free energy change of the ion-pair dissociation is calculated as $\Delta G = \Delta H - T\Delta S$. The free energies and dissociation constants at 298.15 K are shown in Table 1. As can be seen from the table, the Gibbs free energies of all the dissociation reactions are positive. In turn, this means that the Gibbs free energies of the reverse reactions—the ion-pair formation—are negative, and we conclude that ion-pair formation is spontaneous, and rather strongly so, in all three chosen systems. If we compare the dissociation constants of Fc^+−FSI^- with Fc^+−DCA^-, we find that Fc^+−DCA^- has a slightly lower dissociation constant. We alert the reader that a relative trend based on such small energy differences is not conclusive. On the other hand, the comparison between Fc−FSI and Fc−DCA ion-pairing energetics within the same B3LYP-D3 model will include error cancellations which increases the fidelity. The current results indicate that Fc^+ has a stronger interaction with DCA^- than with FSI^- which may be due to the smaller size of DCA^- which brings it geometrically closer to Fc^+ in the ion-pair, resulting in a stronger Coulomb interaction.

Table 1. Gibbs Free Energy Change and Dissociation Constants Predicted at B3LYP-D3/6-311++G//B3LYP-D3/6-31+G* level**

ion pair	solvent	ΔG (eV)	dissociation constants
Fc^+−FSI^-	dichloromethane	0.14	4.14×10^{-3}
Fc^+−DCA^-	dichloromethane	0.17	1.11×10^{-3}
DMB^+−PF_6^-	ethylene carbonate: ethyl methyl carbonate (3:7 volume ratio)	0.24	1.08×10^{-4}

3.3. Electrolyte Concentration Dependence of Redox Potential. To examine the redox potential change as a function of the supporting electrolyte concentration, we use eq 7 where the standard-state redox potential was obtained in section 3.1, and the concentration of the "free" redox active solute at various electrolyte concentrations is deduced from the dissociation constants in Table 1. In the first example system, the redox active solute is $Fc^0/^+$, while the supporting electrolyte is [pmpyr][FSI], and the solvent is dichloromethane. We fixed the concentration of Fc^0 and Fc^+ to 2 mM, which is also the concentration employed in Torriero et al.[25] The supporting salt ([pmpyr][FSI]) concentration ranges from 0.1 to 9.0 M. The simulated relationship is plotted in Figure 3, where, for comparison reasons, the concentration dependence of the $Fc^0/^+$ redox potential on the [bmpyr][DCA] salt is also shown. At low concentrations, an unambiguous logarithmic relationship is manifested. Meanwhile, under neat conditions, the relationship is asymptotically linear. Within the concentration range 4.0 M−9.0 M, the redox potential−concentration data can be fitted to two linear equations $E_{Fc} = -0.0041\cdot[FSI] + 0.41$ and $E_{Fc} = -0.0041\cdot[DCA] + 0.37$, in which, [FSI] and [DCA] are the concentrations of FSI and DCA, respectively. The correlation coefficient R^2 is as high as 0.986.

Compared to the experimental observations by Torriero et al., our predictions are systematically 0.1−0.2 V lower and the predicted change with concentration slightly larger. We predict that the total change in $Fc^0/^+$ redox potential from dilute to neat condition is 0.11 and 0.12 V in [pmpyr][FSI] and

DOI: 10.1021/acs.jctc.6b00289
J. Chem. Theory Comput. 2016, 12, 4501−4508

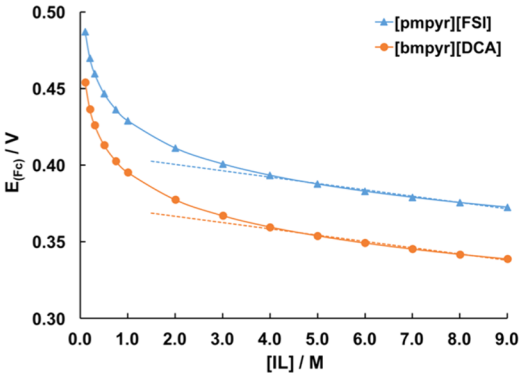

Figure 3. Dependence of the $Fc^0/^+$ redox potential on the concentration of [pmpyr][FSI] and [bmpyr][DCA]. For both electrolytes, dichloromethane is used as the solvent and $DmFc^0/^+$ is used as the reference electrode. Dash lines indicate the linear fitting of the redox potential versus the ionic liquid concentration ranging from 4.0 M to 9.0 M.

[bmpyr][DCA], respectively, while the experimental observed change is less than 0.07 V. Although the exact number differs, the qualitative trend is very well reproduced. Both our simulation and Torriero's experiment shows that (1) the redox potential to reduce Fc^+ in [bmpyr][DCA] is lower than in [pmpyr][FSI]; (2) the concentration dependence follows a logarithmic relationship at low concentrations (<4 M) and (3) the concentration dependence becomes linear at neat conditions (≥4 M). The overall agreement with experiments provides strong evidence that our hypothesis that *the effective formation of ion pairs in the electrolyte causes a change in the redox potential through an equilibrium shift of the concentration of the active species* is correct.

Turning to ferrocene, similarly we find that the direct approach overestimates the influence from ion-pairing with different anions on the solute redox potential. The calculated reduction potentials of Fc^+−FSI and Fc^+−DCA are 0.02 and 0.24 V, respectively. The difference between the two is up to 0.22 V, while experimentally it is only 0.05 V (0.568 V vs 0.564 V).[25] Moreover, the relative order is wrong: the direct ion-pair ionization potential predicts the redox potential of Fc^+−DCA reduction to be higher than Fc^+−FSI reduction; however, experiments exhibit a lower $Fc^{0/+}$ redox potential for [bmpyr]-[DCA] as compared to [pmpyr][FSI]. However, as shown in Figure 3, the IPE scheme proposed here predicts the correct order of the $Fc^0/^+$ redox potentials in [bmpyr][DCA] vs [pmpyr][FSI]. In effect, because the Fc^+−DCA ion-pair exhibits a smaller dissociation constant, it suppresses the population of "free" Fc^+, resulting in a lower redox potential.

Comparing to other proposed methodologies, the proposed IPE model presents an improvement to directly adopting the redox potential of ion pair as the final redox potential[3,10−12] by taking into account the specie (ion-paired or free) that is reduced/oxidized as well as the shift in equilibrium of the electrolyte species. As compared to Seto et al.,[22] in which the effect of the ion-pair was entered indirectly through the dielectric constant of the composite electrolyte, we find two improvements: (i) the linear asymptotic trend at neat conditions is obtained and (ii) the strong dependence on the dielectric constant is removed. Indeed, Seto et al. confirm that the dielectric constant ε remains poorly understood and was assumed to be larger than that of the solvent.

It should be noted that our model still contains several approximations. (1) The chemical activity coefficients γ are taken as constant at 1.0. At high concentrations, this will no longer hold and indeed our predictions at high concentrations retain some logarithmic character rather than the correct linear relationship, which we believe originates from the constant activity coefficients. However, an adjustable set of activity coefficients is straightforward to incorporate. (2) The model does not correct for the basis set superposition error (BSSE).[46−48] In principle, it can be corrected by the counterpoise method (CP)[47,49] and other similar approaches.[50] (3) The choice of continuum solvation model provides a potential bias. In this work, we employed a solvent interface constructed at the van der Waals surface (vdW). An alternative approach would be to use a solvent accessible surface (SAS). However, there is no report showing that SAS performs systematically better than the vdW surface. On the other hand, the vdW surface may favor a too tight solute−solvent interface, especially for small molecules, which may overstabilize the free ion compared to the ion-pair. As a result, it may overestimate the dissociation constant and underestimate the effect on the redox potential. Fortuitously, errors from items 2 and 3 operate oppositely to each other and we expect a partial cancellation. (4) In some cases, the implicit solvent model may be insufficient, and a more sophisticated solvent model should be employed. In such events, the current proposed framework is straightforward to extend using other models for obtaining the Gibbs free energies. Furthermore, we emphasize that the IPE model assumes chemical equilibrium. Hence, dynamic effects, such as diffusion and charge transfers are not taken into account. (5) In the case of organic molecules, for example, $DMB^{0/+}$, the decomposition and side reactions can also play an important role in reduction potential,[51] and we emphasize that such effects are not considered in the current model.

In addition to the above approximations, errors can originate from the B3LYP itself. The error in reaction energy can be quite large, up to 0.8 eV, if, for example, a covalent bond change is involved.[52] However, in ion-pair formation/dissociation processes, the main contributions derive from electrostatic and van der Waals (vdW) interactions which are typically of much smaller magnitude. To capture the delicate change in these noncovalent interactions, we employed Grimme's dispersion correction[32] which has been shown to exhibit a mean absolute deviation (MAD) of 0.02 eV for the binding energy of the S66 noncovalent interaction benchmark set.[53] Compared to the magnitude of the dissociation energies obtained in this work (~0.1−0.2 eV), the estimated error bar is tolerable.

In summary, the IPE model exhibits very good agreement with experimental results, both qualitatively as well as quantitatively. It confirms our initial hypothesis that the ion-pairing influences the redox potential of a solution through the available equilibrium population of the redox active specie (ion-paired or free).

3.4. Application to Battery Redox Shuttle and Organic Redox Follow Batteries. Finally, we apply the proposed IPE approach to an electrolyte system other than the ferrocene-based one. An extensively studied redox active solute is 2,5-di-*tert*-butyl-1,4-bis(2-methoxyethoxy)benene (DBBB)[8,44] which has been suggested as a candidate for battery redox shuttles and nonaqueous redox flow batteries. However, its redox behavior as a function of the concentration of the supporting electrolyte has not been studied, neither experimentally nor computation-

DOI: 10.1021/acs.jctc.6b00289
J. Chem. Theory Comput. 2016, 12, 4501−4508

ally. Here we present our approach on a simplified molecule, 2,5-dimethyl-1,4-bis(2-methoxy)benene (DMB), as a very similar alternative and proxy to DBBB. The structures of the DBBB and DMB are shown in Figure 1. The original electrolyte as used in ref 44 is employed: $LiPF_6$ solvated in a mixture of ethylene carbonate (EC) and ethyle methyl carbonate (EMC) with a 3:7 volume ratio. The redox potential to oxidize DMB^0 to DMB^+ was calculated at the B3LYP-D3/6-31+G* level, yielding 4.34 V vs Li/Li^+. The result should be compared to the experimental value (3.93 V vs Li/Li^+).[8,44] Following the proposed approach we calculate the dependence of the $DMB^{0/+}$ redox potential as a function of the $LiPF_6$ concentration. The result is shown in Figure 4a where we observe that the redox potential changes by 0.12 V within the concentration range 0.1 to 9.0 M, similar to the ferrocene system.

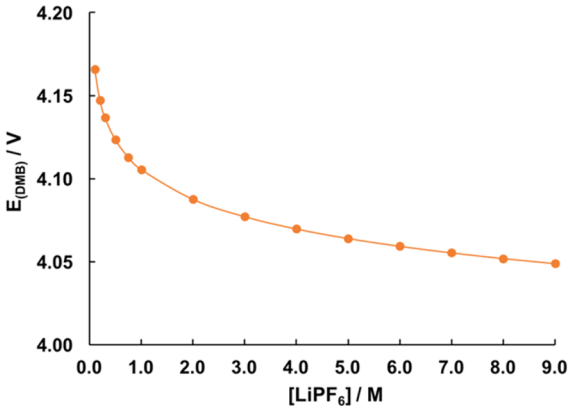

(a)

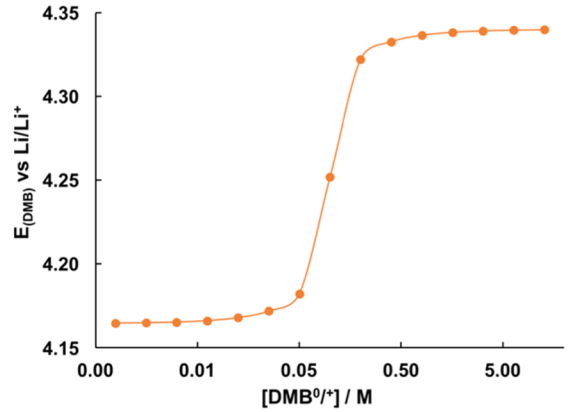

(b)

Figure 4. Calculated concentration dependence of the $DMB^{0/+}$ redox potential in the $LiPF_6$ electrolyte showing (a) the dependence of the DMB^+ reduction potential on the $LiPF_6$ salt concentration and (b) the dependence of the DMB^+ reduction potential on the $DMB^{0/+}$ concentration with the $LiPF_6$ concentration fixed at 0.1 M.

In the context of ion-pair formation, the redox potential is no longer simply linked to the initial concentration of the redox active solute via the Nernst equation. To further explore the concentration dependence behavior, we fix the $LiPF_6$ concentration and vary the $DMB^{0/+}$ concentration to calculate the redox potential of DMB with different initial $DMB^{0/+}$ concentrations. The initial concentrations of DMB^0 and DMB^+ are set to be the same in the simulation. Interestingly, a titration curve style relationship (see Figure 4b) is found. At the beginning ($\leq$0.05 M) the redox potential changes very slowly. The change rate suddenly increases when the concentration approaches 0.1 M, which equals the $LiPF_6$ concentration used in the simulation. At high concentrations (>0.5 M), the change rate decreases again. As can be seen from the figure, the total potential change during the entire concentration range occurs mainly near the equivalence point (e.g., equal concentrations of salt and DMB^+) of the $DMB^+-PF_6^-$ ion-pair formation. Such information provides an opportunity to tune the redox potential of active molecules in the optimization of redox shuttles and redox flow batteries.

4. CONCLUSIONS

We demonstrate a new computational scheme to simulate the dependence of a solute redox potential on the supporting electrolyte concentration. This *ion-pair equilibrium* scheme postulates that the ion-pair formation changes the available amount of the active redox solute and as a consequence changes the redox potential of the solution. Using the methodology, we compare our results to two existing experimental studies: ferrocene[25] and benzoquinone,[22] and find that the agreement is improved as compared to previously proposed methods. A logarithmic behavior on the redox potential is obtained at low salt concentrations, while under neat conditions, the relationship is asymptotically linear. Examining the maximal impact of ion pair formation, we find that equal concentrations of the salt and active redox specie is recommended. The proposed scheme improves our understanding of the impact of ion-pairing on redox active species in solution and can, for example, be used to tune the redox potential by changing the concentration of the supporting electrolyte.

AUTHOR INFORMATION

Corresponding Author

*E-mail: kapersson@lbl.gov.

Funding

Support for this work came from the U.S. Department of Energy, Basic Energy Science, Joint Center for Energy Storage Research under Contract No. DE-AC02-06CH11357. The calculations were performed using the computational resources of the National Energy Research Scientific Computing Center, which is supported by the Office of Science of the U.S. Department of Energy under Contract No. DE-AC02-05CH11231. The Materials Project (BES DOE Grant No. EDCBEE) is acknowledged for infrastructure and algorithmic support.

Notes

The authors declare no competing financial interest.

REFERENCES

(1) Bjerrum, N. J. *Untersuchungen über Ionenassoziation*; Kongelige Danske Videnskabernes Selskab: Copenhagen, Denmark, 1926; No. 9, pp 7.

(2) Marcus, Y.; Hefter, G. Ion Pairing. *Chem. Rev.* **2006**, *106*, 4585−4621.

(3) Rajput, N. N.; Qu, X.; Sa, N.; Burrell, A. K.; Persson, K. A. The Coupling between Stability and Ion Pair Formation in Magnesium Electrolytes from First-Principles Quantum Mechanics and Classical Molecular Dynamics. *J. Am. Chem. Soc.* **2015**, *137*, 3411−3420.

DOI: 10.1021/acs.jctc.6b00289
J. Chem. Theory Comput. 2016, 12, 4501−4508

(4) Petrauskas, V.; Maximowitsch, E.; Matulis, D. Thermodynamics of Ion Pair Formations Between Charged Poly(Amino Acid)s. *J. Phys. Chem. B* **2015**, *119*, 12164−12171.
(5) Seo, D. M.; Reininger, S.; Kutcher, M.; Redmond, K.; Euler, W. B.; Lucht, B. L. Role of Mixed Solvation and Ion Pairing in the Solution Structure of Lithium Ion Battery Electrolytes. *J. Phys. Chem. C* **2015**, *119*, 14038−14046.
(6) Buchner, R.; Chen, T.; Hefter, G. Complexity in "Simple" Electrolyte Solutions: Ion Pairing in MgSO4 (Aq). *J. Phys. Chem. B* **2004**, *108*, 2365−2375.
(7) Zhang, Y.; Maginn, E. J. Direct Correlation between Ionic Liquid Transport Properties and Ion Pair Lifetimes: A Molecular Dynamics Study. *J. Phys. Chem. Lett.* **2015**, *705*, 700−705.
(8) Brushett, F. R.; Vaughey, J. T.; Jansen, A. N. An All-Organic Non-Aqueous Lithium-Ion Redox Flow Battery. *Adv. Energy Mater.* **2012**, *2*, 1390−1396.
(9) Xiong, L.; Fletcher, A. M.; Davies, S. G.; Norman, S. E.; Hardacre, C.; Compton, R. G. Tuning Solute Redox Potentials by Varying the Anion Component of Room Temperature Ionic Liquids. *Chem. Commun.* **2012**, *48*, 5784.
(10) Maeshima, H.; Moriwake, H.; Kuwabara, A.; Fisher, C. a. J. Quantitative Evaluation of Electrochemical Potential Windows of Electrolytes for Electric Double-Layer Capacitors Using Ab Initio Calculations. *J. Electrochem. Soc.* **2010**, *157*, A696.
(11) Maeshima, H.; Moriwake, H.; Kuwabara, a.; Fisher, C. a. J.; Tanaka, I. An Improved Method for Quantitatively Predicting the Electrochemical Stabilities of Organic Liquid Electrolytes Using Ab Initio Calculations. *J. Electrochem. Soc.* **2014**, *161*, G7−G14.
(12) Haskins, J. B.; Bauschlicher, C. W.; Lawson, J. W. Ab Initio Simulations and Electronic Structure of Lithium-Doped Ionic Liquids: Structure, Transport, and Electrochemical Stability. *J. Phys. Chem. B* **2015**, *119*, 14705−14719.
(13) Ong, S. P.; Andreussi, O.; Wu, Y.; Marzari, N.; Ceder, G. Electrochemical Windows of Room-Temperature Ionic Liquids from Molecular Dynamics and Density Functional Theory Calculations. *Chem. Mater.* **2011**, *23*, 2979−2986.
(14) Zhang, Y.; Shi, C.; Brennecke, J. F.; Maginn, E. J. Refined Method for Predicting Electrochemical Windows of Ionic Liquids and Experimental Validation Studies. *J. Phys. Chem. B* **2014**, *118*, 6250−6255.
(15) Fry, A. J.; Hutchins, C. S.; Chung, L. L. Electrolyte Effects upon the Electrochemical Reduction of Cyclooctatetraene in Dimethyl Sulfoxide. *J. Am. Chem. Soc.* **1975**, *97*, 591−595.
(16) Suo, L.; Borodin, O.; Gao, T.; Olguin, M.; Ho, J.; Fan, X.; Luo, C.; Wang, C.; Xu, K. Water-in-Salt" Electrolyte Enables High-Voltage Aqueous Lithium-Ion Chemistries. *Science* **2015**, *350*, 938−943.
(17) Watkins, T.; Kumar, A.; Buttry, D. A. Designer Ionic Liquids for Reversible Electrochemical Deposition/Dissolution of Magnesium. *J. Am. Chem. Soc.* **2016**, *138*, 641−650.
(18) Han, S.-D.; Rajput, N. N.; Qu, X.; Pan, B.; He, M.; Ferrandon, M. S.; Liao, C.; Persson, K. A.; Burrell, A. K. Origin of Electrochemical, Structural, and Transport Properties in Nonaqueous Zinc Electrolytes. *ACS Appl. Mater. Interfaces* **2016**, *8*, 3021−3031.
(19) Jensen, B. S.; Parker, V. D. Reactions of Aromatic Anion Radicals and Dianions. II. Reversible Reduction of Anion Radicals to Dianions. *J. Am. Chem. Soc.* **1975**, *97*, 5211−5217.
(20) Assary, R. S.; Brushett, F. R.; Curtiss, L. A. Reduction Potential Predictions of Some Aromatic Nitrogen-Containing Molecules. *RSC Adv.* **2014**, *4*, 57442−57451.
(21) Namazian, M.; Lin, C. Y.; Coote, M. L. Benchmark Calculations of Absolute Reduction Potential of Ferricinium/ferrocene Couple in Nonaqueous Solutions. *J. Chem. Theory Comput.* **2010**, *6*, 2721−2725.
(22) Seto, K.; Nakayama, T.; Uno, B. Formal Redox Potentials of Organic Molecules in Ionic Liquids on the Basis of Quaternary Nitrogen Cations as Adiabatic Electron Affinities. *J. Phys. Chem. B* **2013**, *117*, 10834−10845.
(23) Tomasi, J.; Mennucci, B.; Cammi, R. Quantum Mechanical Continuum Solvation Models. *Chem. Rev.* **2005**, *105*, 2999−3093.
(24) Cramer, C. J.; Truhlar, D. G. Implicit Solvation Models: Equilibria, Structure, Spectra, and Dynamics. *Chem. Rev.* **1999**, *99*, 2161−2200.
(25) Torriero, A. a J.; Howlett, P. C. Ionic Liquid Effects on the Redox Potential of Ferrocene. *Electrochem. Commun.* **2012**, *16*, 84−87.
(26) Hohenberg, P.; Kohn, W. Inhomogeneous Electron Gas. *Phys. Rev.* **1964**, *136*, B864−B871.
(27) Kohn, W.; Sham, L. J. Self-Consistent Equations Including Exchange and Correlation Effects. *Phys. Rev.* **1965**, *140*, A1133−A1138.
(28) Shao, Y.; Gan, Z.; Epifanovsky, E.; Gilbert, A. T. B.; Wormit, M.; Kussmann, J.; Lange, A. W.; Behn, A.; Deng, J.; Feng, X.; Ghosh, D.; Goldey, M.; Horn, P. R.; Jacobson, L. D.; Kaliman, I.; Khaliullin, R. Z.; Kuś, T.; Landau, A.; Liu, J.; Proynov, E. I.; Rhee, Y. M.; Richard, R. M.; Rohrdanz, M. A.; Steele, R. P.; Sundstrom, E. J.; Woodcock, H. L.; Zimmerman, P. M.; Zuev, D.; Albrecht, B.; Alguire, E.; Austin, B.; Beran, G. J. O.; Bernard, Y. A.; Berquist, E.; Brandhorst, K.; Bravaya, K. B.; Brown, S. T.; Casanova, D.; Chang, C.-M.; Chen, Y.; Chien, S. H.; Closser, K. D.; Crittenden, D. L.; Diedenhofen, M.; DiStasio, R. A.; Do, H.; Dutoi, A. D.; Edgar, R. G.; Fatehi, S.; Fusti-Molnar, L.; Ghysels, A.; Golubeva-Zadorozhnaya, A.; Gomes, J.; Hanson-Heine, M. W. D.; Harbach, P. H. P.; Hauser, A. W.; Hohenstein, E. G.; Holden, Z. C.; Jagau, T.-C.; Ji, H.; Kaduk, B.; Khistyaev, K.; Kim, J.; Kim, J.; King, R. A.; Klunzinger, P.; Kosenkov, D.; Kowalczyk, T.; Krauter, C. M.; Lao, K. U.; Laurent, A. D.; Lawler, K. V.; Levchenko, S. V.; Lin, C. Y.; Liu, F.; Livshits, E.; Lochan, R. C.; Luenser, A.; Manohar, P.; Manzer, S. F.; Mao, S.-P.; Mardirossian, N.; Marenich, A. V.; Maurer, S. A.; Mayhall, N. J.; Neuscamman, E.; Oana, C. M.; Olivares-Amaya, R.; O'Neill, D. P.; Parkhill, J. A.; Perrine, T. M.; Peverati, R.; Prociuk, A.; Rehn, D. R.; Rosta, E.; Russ, N. J.; Sharada, S. M.; Sharma, S.; Small, D. W.; Sodt, A.; Stein, T.; Stück, D.; Su, Y.-C.; Thom, A. J. W.; Tsuchimochi, T.; Vanovschi, V.; Vogt, L.; Vydrov, O.; Wang, T.; Watson, M. A.; Wenzel, J.; White, A.; Williams, C. F.; Yang, J.; Yeganeh, S.; Yost, S. R.; You, Z.-Q.; Zhang, I. Y.; Zhang, X.; Zhao, Y.; Brooks, B. R.; Chan, G. K. L.; Chipman, D. M.; Cramer, C. J.; Goddard, W. A.; Gordon, M. S.; Hehre, W. J.; Klamt, A.; Schaefer, H. F.; Schmidt, M. W.; Sherrill, C. D.; Truhlar, D. G.; Warshel, A.; Xu, X.; Aspuru-Guzik, A.; Baer, R.; Bell, A. T.; Besley, N. A.; Chai, J.-D.; Dreuw, A.; Dunietz, B. D.; Furlani, T. R.; Gwaltney, S. R.; Hsu, C.-P.; Jung, Y.; Kong, J.; Lambrecht, D. S.; Liang, W.; Ochsenfeld, C.; Rassolov, V. A.; Slipchenko, L. V.; Subotnik, J. E.; Van Voorhis, T.; Herbert, J. M.; Krylov, A. I.; Gill, P. M. W.; Head-Gordon, M. Advances in Molecular Quantum Chemistry Contained in the Q-Chem 4 Program Package. *Mol. Phys.* **2015**, *113*, 184−215.
(29) Krylov, A. I.; Gill, P. M. W. Q-Chem: An Engine for Innovation. *Wiley Interdiscip. Rev. Comput. Mol. Sci.* **2013**, *3*, 317−326.
(30) Qu, X.; Jain, A.; Rajput, N. N.; Cheng, L.; Zhang, Y.; Ong, S. P.; Brafman, M.; Maginn, E.; Curtiss, L. A.; Persson, K. A. The Electrolyte Genome Project: A Big Data Approach in Battery Materials Discovery. *Comput. Mater. Sci.* **2015**, *103*, 56−67.
(31) Cheng, L.; Assary, R. S.; Qu, X.; Jain, A.; Ong, S. P.; Rajput, N. N.; Persson, K.; Curtiss, L. A. Accelerating Electrolyte Discovery for Energy Storage with High Throughput Screening. *J. Phys. Chem. Lett.* **2015**, *6*, 283−291.
(32) Grimme, S.; Antony, J.; Ehrlich, S.; Krieg, H. A Consistent and Accurate Ab Initio Parametrization of Density Functional Dispersion Correction (DFT-D) for the 94 Elements H-Pu. *J. Chem. Phys.* **2010**, *132*, 154104.
(33) Goerigk, L.; Grimme, S. A Thorough Benchmark of Density Functional Methods for General Main Group Thermochemistry, Kinetics, and Noncovalent Interactions. *Phys. Chem. Chem. Phys.* **2011**, *13*, 6670.
(34) Stephens, P. J.; Devlin, F. J.; Chabalowski, C. F.; Frisch, M. J. Ab Initio Calculation of Vibrational Absorption and Circular Dichroism Spectra Using Density Functional Force Fields. *J. Phys. Chem.* **1994**, *98*, 11623−11627.
(35) Nicklass, A.; Dolg, M.; Stoll, H.; Preuss, H. Ab Initio Energy-Adjusted Pseudopotentials for the Noble Gases Ne through Xe:

DOI: 10.1021/acs.jctc.6b00289
J. Chem. Theory Comput. 2016, 12, 4501−4508

Calculation of Atomic Dipole and Quadrupole Polarizabilities. *J. Chem. Phys.* **1995**, *102*, 8942.
(36) Tomasi, J.; Mennucci, B.; Cancès, E. The IEF Version of the PCM Solvation Method: An Overview of a New Method Addressed to Study Molecular Solutes at the QM Ab Initio Level. *J. Mol. Struct.: THEOCHEM* **1999**, *464*, 211−226.
(37) Wang, P.; Anderko, A. Computation of Dielectric Constants of Solvent Mixtures and Electrolyte Solutions. *Fluid Phase Equilib.* **2001**, *186*, 103−122.
(38) Kirkwood, J. G. The Dielectric Polarization of Polar Liquids. *J. Chem. Phys.* **1939**, *7*, 911.
(39) Bard, A. J.; Parsons, R.; Jordan, J. *Standard Potentials in Aqueous Solution*; CRC Press: New York, 1985; pp 1−4.
(40) IUPAC. In *Compendium of Chemical Terminology*, 2nd ed.; McNaught, A. D., Wilkinson, A., Eds.; Blackwell Scientific Publications: Oxford, 1997; pp 473.
(41) Nguyen, K.-L.; Dionne, E. R.; Badia, A. Redox-Controlled Ion-Pairing Association of Anionic Surfactant to Ferrocene-Terminated Self-Assembled Monolayers. *Langmuir* **2015**, *31*, 6385−6394.
(42) Grotzinger, C.; Burget, D.; Jacques, P.; Fouassier, J. P. A Novel and Efficient Xanthenic Dye-Organometallic Ion-Pair Complex for Photoinitiating Polymerization. *J. Appl. Polym. Sci.* **2001**, *81*, 2368−2376.
(43) Carter, T. J.; Mohtadi, R.; Arthur, T. S.; Mizuno, F.; Zhang, R.; Shirai, S.; Kampf, J. W. Boron Clusters as Highly Stable Magnesium-Battery Electrolytes. *Angew. Chem., Int. Ed.* **2014**, *53*, 3173−3177.
(44) Zhang, L.; Zhang, Z.; Redfern, P. C.; Curtiss, L. a.; Amine, K. Molecular Engineering towards Safer Lithium-Ion Batteries: A Highly Stable and Compatible Redox Shuttle for Overcharge Protection. *Energy Environ. Sci.* **2012**, *5*, 8204.
(45) Aranzaes, J. R.; Daniel, M.-C.; Astruc, D. Metallocenes as References for the Determination of Redox Potentials by Cyclic Voltammetry - Permethylated Iron and Cobalt Sandwich Complexes, Inhibition by Polyamine Dendrimers, and the Role of Hydroxy-Containing Ferrocenes. *Can. J. Chem.* **2006**, *84*, 288−299.
(46) Balabin, R. M. Enthalpy Difference between Conformations of Normal Alkanes: Intramolecular Basis Set Superposition Error (BSSE) in the Case of N-Butane and N-Hexane. *J. Chem. Phys.* **2008**, *129*, 164101.
(47) Paizs, B.; Suhai, S.; Biophysics, M.; Cancer, G.; Feld, I. N. Comparative Study of BSSE Correction Methods at DFT and MP2 Levels of Theory. *J. Comput. Chem.* **1998**, *19*, 575−584.
(48) Hobza, P.; Müller-Dethlefs, K. *Non-Covalent Interactions: Theory and Experiment*; Royal Society of Chemistry: Cambridge, England, 2010; pp 13.
(49) van Duijneveldt, F. B.; van Duijneveldt-van de Rijdt, J. G. C. M.; van Lenthe, J. H. State of the Art in Counterpoise Theory. *Chem. Rev.* **1994**, *94*, 1873−1885.
(50) Mayer, I. Towards a "Chemical" Hamiltonian. *Int. J. Quantum Chem.* **1983**, *23*, 341−363.
(51) Borodin, O.; Behl, W.; Jow, T. R. Oxidative Stability and Initial Decomposition Reactions of Carbonate, Sulfone, and Alkyl Phosphate-Based Electrolytes. *J. Phys. Chem. C* **2013**, *117*, 8661−8682.
(52) Check, C. E.; Gilbert, T. M. Progressive Systematic Underestimation of Reaction Energies by the B3LYP Model as the Number of C−C Bonds Increases: Why Organic Chemists Should Use Multiple DFT Models for Calculations Involving Polycarbon Hydrocarbons. *J. Org. Chem.* **2005**, *70*, 9828−9834.
(53) van Santen, J. a; DiLabio, G. a. Dispersion Corrections Improve the Accuracy of Both Noncovalent and Covalent Interactions Energies Predicted by a Density-Functional Theory Approximation. *J. Phys. Chem. A* **2015**, *119*, 6703−6713.

DOI: 10.1021/acs.jctc.6b00289
J. Chem. Theory Comput. 2016, 12, 4501−4508